Research Square

Preprints are preliminary reports that have not undergone peer review.
They should not be considered conclusive, used to inform clinical practice,
or referenced by the media as validated information.

Bio-based coating for wool fabrics prepared from sodium alginate and Eobania Vermiculata snail shell waste to improve flammability properties

khadija haddaji
University of Monastir: Textile Engineering Laboratory (LGTEX), LR11ES42,5070, Ksar Hellal, Tunisia
Rim Cheriaa
cheriaar@yahoo.fr

University of Monastir: Higher Institut of Fashion of Monastir, 5000, Monastir, Tunisia
Soumaya Tabib
University of Monastir, National School of Engineers of Monastir, (ENIM), 5000, Monastir, Tunisia
Boubaker Jaouachi
University of Monastir: National School of Engineers (ENIM), 5000, Monastir, Tunisia

Research Article

Keywords: Wool fabric, bio-based coating, Eobania Vermiculata snail shell waste, sodium alginate bio-polymer, flammability properties, physicochemical and mechanical characterization

Posted Date: March 24th, 2026

DOI: https://doi.org/10.21203/rs.3.rs-9057223/v1

License: This work is licensed under a Creative Commons Attribution 4.0 International License.
Read Full License

Version of Record: A version of this preprint was published at Environmental Science and Pollution Research on June 12th, 2026. See the published version at https://doi.org/10.1007/s11356-026-37911-9.

BIO-BASED COATING FOR WOOL FABRICS PREPARED FROM SODIUM ALGINATE AND *EOBANIA VERMICULATA* SNAIL SHELL WASTE TO IMPROVE FLAMMABILITY PROPERTIES

Khadija Haddaji[1,2], Rim cheriaa[1,3], Soumaya Tabib[2], and Boubaker Jaouachi[1,2]*

[1] University of Monastir, Textile Engineering Laboratory (LGTex), LR11ES42, 5070, Ksar Hellal, Tunisia.
[2] University of Monastir, National School of Engineers of Monastir (ENIM), 5000, Monastir, Tunisia.
[3] University of Monastir, Higher Institute of Fashion of Monastir, 5000, Monastir, Tunisia.

[(*)] Correspondence: cheriaar@yahoo.fr

Abstract

This study investigates the development of a new sustainable bio-based coating to improve flammability properties of wool fabrics. The treatment contains a hybrid formula composed of *Eobania Vermiculata* (EV) snail shell microparticles rich in non-combustible calcium carbonate ($CaCO_3$) and mineral content and sodium alginate (SA) used as a bio thickener. The direct coating method is used for the application. Vertical flammability tests demonstrated that coated fabric burning ceased before the ignition source was removed (12s). The char length decreased from 27.53 ± 4.27 cm in the untreated wool fabric (Wool-NT) to 5.4 ± 0.03 cm in the fabric treated with SA and EV snail shell microparticles (Wool-SA-EV). SEM images show a relatively smooth fiber surface due to SA thickener and distributed snail shell microparticles with different microparticle forms and sizes (< 90 μm). FTIR results confirmed, through the characteristic bands, the deposition of the treatment on the fabric surface through physical modifications. The increase in the tensile strength of Wool-SA-EV samples compared to the non-treated samples is of about (16.6%) with a significant increase in elastic strain and in elongation at maximum force (85.4%). Results highlight the feasibility of using an agrowaste to create an eco-friendly and bio-based coating for wool fabrics.

KEYWORDS: Wool fabric, bio-based coating, *Eobania Vermiculata* snail shell waste, sodium alginate bio-polymer, flammability properties, physicochemical and mechanical characterization

1. Introduction

Several chemical formulations have been proposed for the preparation of flame retardants (FRs). Various types of FRs are classified into two types based on their composition, namely, halogenated (bromo and chloro derivatives), and non-halogenated (nitrogen-based FRs, boron-based FRs, metal hydroxide-based FRs, flavonoid-based FRs, and phosphorus-based FRs) (Sykam et al. 2021).

In view of environmental protection issues, interest has grown in research involving ecological flame retardants based on natural substances. Chitosan (Shahidi et al. 2015), phytic acid (Sykam et al. 2021), borate-functionalized caramel (Cheng et al. 2021), phytate derivative (Cheng et al. 2022) and many others were applied as potential FR materials for wool fabrics. Durability is, however, questionable (Mathur et al. 2020; Wang et al. 2021).

Wool, a natural protein fiber, is widely used in clothing, home textiles, and industrial garments due to its comfort and naturally high level of fire resistance. Wool fibers have a high limiting oxygen index (LOI) of 25-26% and an ignition temperature up to 570-600 °C (Ren et al. 2026). Wool's excellent fire resistance characteristics are related to its high content of nitrogen (15-16%) and sulfur (3-4%), its high moisture content (10-14%), and its low combustion temperature (Cardamone 2013). Although wool is a natural fiber commonly used and appreciated for its thermal properties and comfort, its fire-retardant properties limit specific technical and protective uses. In fact, the majority of wool fabrics can perform the horizontal test but are not able for the 45° test or the vertical test. Particular products, such as seat coverings in automobiles and buses, airplane interiors and coverings, mural coverings used in public buildings, safety garments, and long-pile carpets require, further treatment to enhance their fire resistance (Flambard et al. 2005). Once the wool fabric gets ignited, the flame propagates rapidly, resulting in significant property damage and posing to life-threatening risks. Therefore, improving the flame retardancy of wool fabrics is crucial to reduce combustion-related losses [Ren et al. 2026).

Snail shells, which are the bio-shell waste that is abandoned by restaurants or snail merchants, pose a huge environmental problem, despite having little to no market value (Adepitan et al. 2025). Howover, snail shells have shown promise in a variety of applications, including agriculture (soil pH, nutrient uptake), construction (cement additive, self-healing concrete) (Diharjo et al. 2024), biomedicine (bone repair, drug carriers, vaccine delivery) (Janarthanan and Senthil Kumar 2019; Mariadoss et al. 2026), water treatment (bio-adsorbent), and biodiesel production (active nano-catalyst) (Adepitan et al. 2025). Besides, snail shells, rich in non-combustible calcium carbonate ($CaCO_3$), are being researched as sustainable, natural flame retardants for polymers (rubber) and for composites (Diharjo et al. 2024). They reduce fire risk by releasing non-flammable CO_2 (Equation 1), acting as a natural fire extinguisher, and forming protective char due to the mineral content, which helps to form a stable char layer on the material's surface.

$$CaCO_{3(g)} \rightarrow CO_{2(g)} + CaO_{(s)} \quad (1)$$

To the best of our knowledge, research regarding the application of snail shell waste on wool fibers or fabrics are limited. But, Diharjo et al. (2024) proposed a *Ceiba petandra* fiber/ snail powder reinforced polyester composites. Snail powder filler concentration enhanced the tensile strength and the heat resistance of the composite. The percentage of char yield and the limitation index oxygen (LOI) increased as the snail powder filler increased. The flame rate of the composite decreased because the snail powder filler impeded the movement of oxygen and flammable gas. Despite its apparent benefits as a bio-based flame retardant mainly in composite structures (Rungpin et al. 2015; Peceno et al. 2025), snail shell exhibit poor adhesion to textile surface, propably because of particles' structure, size, form, and application technology (Su et al. 2017). This is why it is necessary to choose the suitable intermediary between textile and snail shells particles.

Sodium alginate (SA), a biopolymer, is a water-soluble form of alginate that is commonly used as a thickening agent. It is a natural anionic polysaccharide found in brown algae (*Laminaria Digitata, Ascophyllum Nodosum,*

Macrocystis Pyrifera...) and from diverse bacterial species: (*Azotobacter and Pseudomonas).* Sodium alginate is a polyanionic copolymer made from β-D-mannuronic acid and α-L-guluronic acid via (1→4) glycoside linkages. Its chemical formula is $(C_6H_7NaO_6)_n$, with an average molecular weight of 216.121 g/mol (Sharma and Singh 2025). Sodium alginate solid powder is white and hydrophilic. It dissolves readly in water and can form gels when divalent ions are present. The viscosity of alginate solutions depends on the molecular mass and pH of the reaction mass. The viscosity rises as the pH drops and peaks between pH 3-3.5. In fact, the carboxyl groups get protonated and have the ability to form hydrogen bonds (Wang et al. 2025). SA dissolves slowly in cold water, resulting in a viscous solution. It is insoluble in alcohol, chloroform, and ether. The pH, molecular weight, ionic strength, type of ions in the structure, and concentration all affect solubility (Frent et al. 2022).

Few authors have discussed the treatment of wool with sodium alginates: Azam et al. (2024) proposed a hydrogel composite made from nonwoven wool fabric combined with alginate, gum Arabic, and xanthan gum to assess its performance in adsorbing lead from aqueous solutions. The composite has shown potential for removing Pb^{2+} ions from wastewater. The research of Szczepanik et al. (2025) investigate the idea of incorporating waste sheep wool fibers into a hydrogel to creat a stable material that could enhance water retention and serve as a fertilizer material. An et al. (2020) proposed a process based on a protease enzyme and SA for wool fabric inkjet printing. The results demonstrated a printed treated wool fabrics with higher color performance. On the fiber surfaces, the SA produced homogeneous compact films with improved hydrophilicity of 70.1° contact angle and wetting duration of 3.5 s. The treated fabric shows also acceptable strength, rubbing and washing fastness. In the study of Sadeghi-Kiakhani et al. (2021), wool yarns were grafted with SA - Silver nanoparticles Ag NPs and then dyed with *Cochineal* or *Madder*. The results indicated that the proposed treatment increased the number of dye adsorption sites, thereby enhancing the intermolecular interactions between the natural dyes and the wool fibers. In addition, the pretreatment process enhanced the antimicrobial and antioxidant activities of the wool yarns, with efficiencies exceeding 70%.

Flame retardant treatments were applied to the fabrics' surfaces using a variety of methods, including impregnating the surface of the fabrics by sol-gel process, grafting onto the surface (Ren et al. 2026), layer-by-layer (LbL) assembly (Malucelli 2020), and dip-coating technologies (Sykam et al. 2021). Coating, the process used in our study, consists of spreading chemical solutions to one or both sides of textile fabric in order to enhance their aesthetic, physical qualities, and mechanical properties, and combine the benefits of films, polymers, foams, and fabrics. Three important factors for a feasible coating procedure are: the composition and the structure of the coating textile, the composition of the coating, and the article's final use. The coating's adhesion and its durability are determined by the interaction between the coating and the substrate.

In our previous works, a clear discussion of the physicochemical and thermal properties of *Eobania Vermiculata* (EV) snail shell using optical microscopy observations, Fourier Transform Infrared spectroscopy (FTIR), X-Ray Fluorescence spectrometry (XRF), Thermogravimetric analysis (TGA/DTA), and Differential Scanning Calorimetry (DSC) was presented (Haddaji et al. 2025).

The novelty of the present work is a new coating agent for wool fabrics synthesized from a biopolymer (SA) and an agrowaste (EV snail shell microparticles), which, when blended, form a coating that exhibits improved fire-resistant and probably others. The process described in this study is considered a green approach. The experimental work encompasses the characterization of the materials and the characterization of the coated

substrates in terms of flammability, surface morphology, tensile properties, flexural rigidity, and air permeability. A detailed discussion of the coating method followed is provided in this paper.

2. Experimental Materials and Methods

2.1. Materials

A pretreated plain woven wool fabric (233 g/m²) was supplied by SCD enterprises LTD, UK.

EV snails were collected from vegetation covers located in the north of Tunisia, in December.

Eobania vermiculata is a land snail that can be considered a harmful agricultural pest and can cause great damage to many species of plants. These useless and harmful land snails in many places are collected, used for commercial food, or burnt.

Sodium alginate (CAS NO: 9005-38-3; a beige powder with a purity of 95%) was purchased from CARLO ERBA Reagent. DAZIT Group (France) in this work.

2.2. Preparation of *Eobania Vermiculata* shell powder

The *Eobania Vermiculata* shells were thoroughly cleaned to remove soft tissues and sand, etc. They were immersed in distilled water, rinsed several times to assure cleanliness, and dried in an oven at 60°C (Karaoui et al. 2023). Next, the snail shells were hammered into smaller particles and ground into fine powder using a high-speed blender. Particles were passed through a 90 µm mesh sieve, and only those smaller than 90 µm were selected for the experiments. Snail powder was stored in an airtight plastic bag until it was ready for tests.

2.3. Coating preparation

25 g of SA powder was added into 1 L distilled water at a neutral pH and at 25°C and stirred at 400 rpm for 20 minutes until completely dissolved to obtain a homogeneous solution containing 2.5% (w/v) SA. 20 g of snail shell microparticles were then mixed with SA solution 2% (w/v), and kept under magnetic stirring to ensure complete homogenization. The prepared paste was then stored at room temperature for 24 h to eliminate air bubbles.

2.4. Coating application

Coating trials were conducted using a hand-directed coating technique. A rubber squeegee with square, soft durometer blade and wood grip is used. 6 g of the obtained solution is applied on the front side of the fabric (30 × 7.5 cm). The homogenized coating paste is spread manually one time over the entire fabric stretched over a frame to achieve the desired coating thickness and finally oven dried at 80°C for 5 minutes. One typical advantage of this coating method is that fibers are not stressed during such a process (Jaouachi et al. 2021). It requires a skilled and well-trained operator to ensure reproducibility.

Fig. 1 Schematic illustration of coating process

The add-on percentage on the fabrics was measured using equation (2):

$$\text{Add-On } \% = \frac{M_2 - M_1}{M_1} \times 100 \quad (2)$$

where: M_2, surface weight of coated fabric (g/m^2); M_1, surface weight of uncoated fabric (g/m^2). The obtained results are an average of five tests in each case.

Diverse coated fabrics with distinct coating compositions and their respective codes were presented in table 1:

Table 1. Coated wool fabrics caracteristics and sample code

2.5. Characterization

- Flammability assessment: The flame resistance testing were conducted according to ASTM D6413-2015 (Standard test method for flame resistance of textiles (vertical test)). The treated samples (30 cm × 7.5 cm) were fixed vertically onto a metallic template within a fume hood. Each sample was exposured to the flame of a Bunsen burner for 12 seconds, maintaining a distance of 1 cm from the sample and a flame height of 3.8 cm. The afterflame time (s), the afterglow time, the char length (cm), and the observed burning rate (cm/s) were recorded (Islam et al. 2024; Shikder et al. 2023).

To assess the washing fastness of the treated wool fabrics, coated samples were impregnated in the aqueous solution containing 0.15 wt % of standard detergent at 40 °C for 40 min. The samples were then rinsed for 5 min and dried at 80°C for 4 min.

- Scanning electron microscopy (SEM): The morphology of the coated samples was performed using a scanning electron microscopy VHX-6000, operating at (5 kV). The surface views of the coated fabrics were taken at magnifications of 40× and 90×.

- Fourier transform infrared spectroscopy (FTIR) analysis

Treated fabric specimens were analyzed using the Perkin Elmer Spectrum (Perkin Elmer Inc., Waltham, MA, USA). SA powder and EV microparticles were also tested. Measurements were carried out at room temperature. Since the samples were solid, they were firstly deposited on the top surface of the crystal. Then, the gripper plate was placed on the sample, and the pressure exerted to the gripper plate was adjusted to guarantee uniform contact between the crystal and the sample. The spectra were recorded at a resolution of 4 cm^{-1} over a 4000-500 cm^{-1} wavenumber range with 32 scans.

- Strength properties analysis: The tensile strength of coated samples (50 mm ± 0.5 mm × 200 mm dimensions) was evaluated by a testing machine, Lloyd LR 5 k, as per the ISO 13934-1: 2013 method (Determination of maximum strength and elongation at maximum strength using the strip method). The load cell was 5 kN and the extension speed was set at 100 mm/min.

- Flexural rigidity analysis: Sample flexural rigidity G (mg.cm) is determined from bending length measured according to BS 3356: 1990 (Method for determination of bending length and flexural rigidity of fabrics) and using equation (3).

$$G = M \times C^3 \quad (3)$$

where C: is the bending length (cm), and M: is the fabric mass per unit area (mg.cm^{-2}).

- Thickness analysis: The thickness of fabrics was tested according to ISO 5048-1996 (Method for thickness of textile materials) exerting a pressure of 1 kPa.

- Air permeability analysis: Air permeability tests were measured for uncoated and coated fabrics using an air permeability instrument (supplied by SDL Atlas Textile Testing Solutions) with a head area of 20 cm^2. The air flow passing was measured at 100 Pa pressure according to ISO 9237: 1995 (Determination of the permeability of fabrics to air).

- **Coating contribution:** Equation 4 presents the contribution of the coating $|C|_X$ (%)on the studied property X as a function of the measured property of uncoated fabric X_{uc} and the measured property of coated fabric X_c.

$$|C|_X\ (\%) = 100 \times \frac{X_c - X_{uc}}{X_{uc}} \quad (4)$$

All measurements were repeated five times. Various tests were carried out under textile standard conditions specified in ISO 139: 2005 (Standard atmospheres for conditioning and testing): a temperature of 20 ± 2°C and a relative humidity of 65 ± 4%.

3. Results and Discussions

3.1. Flammability test results

According to ASTM D6413-2015, afterflame time is the duration that a material continues to flame after the ignition source is eliminated. Char length, is the distance between the fabric edge exposed to the flame and the furthest point of apparent fabric damage after a specified tearing force has been applied (Wulandari et al. 2024).

Table 2. Photos of uncoated and coated wool fabrics

Table 2 shows that the control wool fabric (Wool-NT) burned out almost completely during the vertical flammability test, demonstrating a full char length of about 27.53 ± 4.27 cm, a afterflame time of about 32.17 ± 0.52 s, and an observed burning rate of about 0.86 ± 0.33.

Table 3. Flammability testing results

Compared with the Wool-NT fabric, the coated wool fabrics show significantly lower char length: 7.5 ± 0.84 cm for Wool-SA and 5.4 ± 0.03 cm for Wool-SA-EV (Table 3). Fabric burning stoped before the ignition source was removed; thus the treated fabrics also had no afterflame time and afterglowtime, and the treated samples burned less, as is clear in table 2. These results show that the SA coating can significantly improve flame retardancy. In fact, sodium alginate's flame retardancy functions through both gaseous and condensed phases mechanisms. In the gaseous phase, non-flammable gases (e.g., NH_3) emitted during decomposition dilute the concentrations of flammable gases and impede combustion chain reactions by radical quenching, wherein PO· radicals scavenge reactive ·OH and ·H radicals.

In the condensed phase, pyrolysis produces a dense carbon layer that serves as a protective barrier, efficiently insulating against oxygen diffusion and heat transfer (Wang et al. 2025).

Incorporating microparticles of EV snail shell further augments flame retardancy by decreasing char length.

Wool-SA-EV samples were washed, dried, conditioned, and then flammability tests were carried out. Washed Wool-SA-EV samples take back the same flammability properties as uncoated fabric explained by the large difference in solubility of SA and EV snail shell particles and the amount of SA eliminated by the action of water during washing.

3.2. Coated fabric surface morphology

Scanning electron micrographs of coated wool fabrics are given in figure 2. It is seen that the wool fabric coated with SA shows a smooth layer and continuous surface without agglomerations (Figure 2-(b)). SA coating forms a matrix around the wool fibers, which could influence water absorption and filtration properties (Wang et al. 2025). Ahmad et al. (2021) confirmed that the solution of SA can diffuse into the wool fabric due to its porous structure and high absorption capacity of wool fibers.

Fig. 1 SEM images of uncoated and coated wool fabrics

(a) Wool-NT (×40), (b) Wool-SA (×40), (c) Wool-SA-EV (×40), (d) Wool-SA-EV (×90).

Figures 2(c) and 2(d) show that snail shell particles were distributed all over the fabrics, and particle size was different (< 90 μm). The introduction of EV shell microparticles to the wool fabric sample has made the coated surface less smooth due to the presence of microparticles. Particulates of snail shell apparently adhere to the fiber's surface. According to Su et al. (2017), EV microparticle surfaces have an uneven microstructure and a uniform distribution of calcium carbonate seeds. The presence of rod-shaped calcium carbonate seeds shows the existence of aragonite phases of the orthorhombic crystal structure of CaCO. No agglomerations have been detected in figure 2(d) which can be a consequence of the intimate presence of two compounds, such as SA and EV in the coating matrix having significant differences in their solubility parameter according to Salmeia et al. (2016).

3.3. FTIR spectra analysis

The FTIR spectrum of SA powder has been recorded in the range from 4000 to 500 cm^{-1} and presented in figure 3.

Fig. 2 FTIR analysis of sodium alginate powder (SA)

Figure 3 shows the characteristic peaks of SA, which occurred at 3315 cm^{-1}, 2918 cm^{-1}, 1598 cm^{-1}, and 1412 cm^{-1}, corresponding to the O-H stretching vibrations, C-H banding, and asymmetric and symmetric stretching vibrations of $-COO^-$, respectively (Sethi and Manik 2018; Ivanovska et al. 2024). The wide band at 1100 cm^{-1} and 1030 cm^{-1} is assigned to the stretching vibration of COC groups (Wang et al. 2022).

FTIR spectrum of EV snail shell is presented in figure 4.

Fig. 3 FTIR analysis of *Eobania Vermiculata* snail shell

The infrared spectrum of the EVSP displays a peak at 3313 cm^{-1} indicating -OH stretching relative to the moisture vibration mode in the sample. The FTIR spectrum indicates lower intensity organic bands; the band at

1787 cm^{-1} corresponds to the carboxylate groups of the acidic proteins. Four bands characteristic of aragonite, corresponding to the CO_3^{-2} ions, were identified: ν1 at 1083 cm^{-1}, ν2 at 855 cm^{-1}, ν3 at 1455 cm^{-1}, and ν4 at 700-712 cm^{-1}. The ν1 band corresponds to the symmetric stretch mode, and the ν4 band corresponds to the planar flexion mode of carbonate vibration. The characteristic carbonate ν4 bands of aragonite at 712 and 700 cm^{-1} and the characteristic carbonate ν2 band of aragonite at 855 cm^{-1} confirmed the presence of aragonite form of calcium carbonate in the snail shell (Parveen et al. 2020; Haddaji et al. 2025).

Fig. 4 FTIR analysis of uncoated and coated wool fabrics

As can be seen from figure 5, the spectrum of uncoated wool fibers showed a broad absorption peak at around 3275 cm^{-1} attributed to N-H bending vibrations from the amide A linkages, and O-H stretching vibrations from absorbed water. The bands' absorption peak at 2938 cm^{-1} is associated with the symmetrical and asymmetrical stretching vibrations of the CH_2 and CH_3 groups (Belukhina et al. 2021).

Amide bands were also observed at 1636, 1524, and 1238 cm^{-1}. The absorbance peaks at 1636 and 1238 cm^{-1} are assigned, respectively, to the stretching vibrations of C=O bond from amide I and of C-N from amide III. The absorbance peak that appeared at 1524^{-1} cm is assigned to N-H in-plane bending in amide II linkages (Zhang et al. 2018). The weak band with peak at 1067 cm^{-1} refers to the C-H in-plane bending. The very weak band in the lower spectrum region reveals the presence of a disulfide bond, a typical covalent bond of protein molecules, through the stretching vibrational mode, giving more evidence of the presence of wool fibers (Linhares et al. 2023).

A comparison of FTIR spectra between control (Wool-NT) and Wool-SA and Wool-SA-EV revealed similar appearances with a decrease of transmittance percentages. In the transmission spectrum of Wool-SA sample, the peaks at 1431 cm^{-1}, and 3277 cm^{-1} represent the $-COO^-$, and $-OH^-$ functional groups, characteristic groups of alginate in the wool fabric (Ahmad et al. 2021). Compared to Wool-SA transmission spectrum, that of Wool-SA-EV sample shows a new smal peak at 853 cm^{-1} relative to aragonite, more precisely, to the CO_3^{2-} ions. A slight band shift from 1158 cm^{-1} to 1194 cm^{-1} would typically indicate a weakening of intermolecular interactions or a change in molecular environment, often related to hydrogen bonding or coordination, suggesting the functional group C-N stretch in that region is becoming less polar.

3.4. Tensile testing results

The results obtained from the tensile strength according to ISO 13934-1: 2013 are as follows: The maximum force for breakdown recorded when the test specimen is taken to rupture during a tensile test under the specified conditions, and elongation at maximum force is the elongation of the test specimen produced by the maximum force. The tensile test results are summarized in figure 6.

Fig. 5 Tensile strength testing results (warp direction):

(a) Tensile curve, (b) Maximum force, (c) Elongation at maximum force

As shown in figure 6(a), the tensile curves of Wool-NT and Wool- SA showed the same trend, there was only a small difference in maximum elongation, which was mainly related to the structural changes of the fabric after SA coating. The elongation at peak increased from 25.4% for the untreated wool samples (Wool-NT) to 37.6%

for Wool-SA samples (figure 6(c)). Usually, the fabric coated with a polymer shows an improved tensile strength due to the reinforcement. The elongation decreased as the extensibility of the fabric is limited by the bonded polymeric coating (Hassan 2018). However, in our case, we observed that the SA coating increased the elongation of the wool fabric. The results suggest that the SA polymer formed an elastomeric coating on the surface of wool fabric, resulting in increasing the elongation of the fabric.

On the other hand, the level of increase in the tensile strength is quite small in Wool-SA-EV samples compared to the non-treated samples (about 16.6%) with a significant increase in elastic strain (about 10%) and in elongation at maximum force (figure 6(b)). The contribution of the SA-EV coating to the increase of elongation at maximum force is about $|C|_{\text{Elongation at maximum force}} = 85.4\%$.

According to these results, it is surmised that the coating based on SA or SA-EV did not cause any notable damage to the tested wool fabric. In most cases of application of conventional and commercial flame retardant finishes, a significant loss of tensile strength occurred (Islam et al. 2024).

3.5. Flexural rigidity results

The compared results of flexural rigidity of different coated wool fabrics are shown in Table 4. The thickness and the mass per unit area of each sample were also determined by averaging five measurements. Flexural rigidity is calculated based on the average of the bending lengths of the side and backside of the fabric.

Table 4. Comparative flexural rigidity results and structural properties

Table 4 indicates that Wool-SA samples become thicker compared to uncoated fabric. The addition of EV microparticles did not modify the fabric thickness. This result can be explained by the fact that EV microparticles integrate into the interfiber and interyarn spaces, as seen in figure 2(d). The mass per unit area increases from 223.83 ± 1.75 g/m^2 for the uncoated fabric to 235.74 ± 2.13 g/m^2 for Wool -SA-EV which is explained by the fabtric add on % of about 5.41 ± 1.98%. Low values of standard deviation prove that the distribution of the coatings on the fabric is uniform and that the method of application adopted is reproducible.
It is also obvious that the bending rigidity of untreated fabric increased with SA coating. The flexural rigidity of untreated fabric increases from 3.12 ± 0.5 mg.cm to 6.64 ± 0.56 mg.cm in Wool-SA fabric. So, the contribution of the SA coating to the increase of flexural rigidity is about $|C|_{\text{Flexural rigidity}} = 112.8\%$. These results are in accordance with many others, which explained that coating fills the spaces between the yarns and cements the warp and weft threads together, which rigidifies the fabric structure (Jaouachi et al. 2021). It is also noticed that the coating based on SA-EV did not cause any notable modification of wool fabric flexural rigidity.

3.6. Air permeability test results

Air permeability is one of the important properties in the performance of fabrics: clothing indicator of the breathability of finished fabrics. In this experiment, the air permeability of the uncoated and the coated wool samples was measured. Both sides of each fabric sample were subjected to an air permeability test, and the average results were summarized in Table 5:

Table 5. Air permeability test results

Referring to these findings, air permeability for uncoated fabric Wool-NT, coated fabrics Wool-SA, and Wool-SA-EV was estimated 267, 212.33, 165.33 $L/m^2/s$, respectively. It can be concluded that the considered coatings have led to a decrease in the air permeability of about 20% and 38%, respectively. In fact, plain woven fabric is considered as a hierarchical porous structure. The coating material fills the natural pores and interfiber and interyarn spaces, creating a barrier that restricts airflow. As a result, pore distribution, sizes, and shapes were modified. Besides, a more compact structure with blocked yarns was obtained, which is a common finding in studies on functional textiles, waterproofing, and smart fabrics. While this reduces breathability, it often enhances water resistance, windproofing, and thermal insulation, making it useful for technical apparel (Xu et al. 2019).

4. Conclusion

The aim of this research was to develop a coated wool woven fabric, based on *Eobania Vermiculata* snail shell waste and sodium alginate, that can enhance flame resistance using a simple and eco-friendly process.

For this purpose, an aqueous dispersion comprising 20 g/L of EV snail shell microparticles and 25 g/L SA powder as a thickener was prepared and applied on the fabric surface with a direct coating method. For both uncoated and coated samples, flammability assessment, surface morphology, infrared spectrum, tensile strength properties, mass per unit area ($g.m^{-2}$), thickness (mm) coating add-on %, flexural rigidity (mg.cm), and air permeability ($L/m^2/s$) were evaluated.

The treated wool fabrics showed obviously improved FR performance. In fact, the treated fabrics exhibited significantly reduced char length. Compared with the Wool-NT fabric, which has a char length of about 27.53 ± 4.27 cm, the coated Wool-SA samples show a lower char length of about 7.5 ± 0.84 cm and the coated Wool-SA-EV samples a char length of about 5.4 ± 0.03 cm. However, FR effect was not resistant to washing. This presumably raises concerns regarding the coating parameters as well as SA solubility after washing.

The presence of SA coating onto wool fabric was confirmed through SEM micrographs, where snail shell microparticles were distributed all over the fabric, with different particle sizes (<90µm) and forms.

The infrared spectrum analysis of the different peaks of untreated wool fabric Wool-NT was detected in Wool-SA and Wool-SA-EV spectrums. In the transmission spectrum of Wool-SA sample, the peaks at 1431 cm^{-1}, and 3277 cm^{-1} assigned to the $–COO^-$, and $–OH^-$ functional groups, respectively, confirm the presence of alginate in the wool fabric. Wool-SA-EV spectrum shows a new small peak at 853 cm^{-1} relative to aragonite (CO_3^{2-} ions). A slight band shift from 1158 cm^{-1} to 1194 cm^{-1} indicated a weakening of intermolecular interactions or a modification in the molecular environment, typically related to hydrogen bonding or coordination. This suggests that the functional group C–N stretch in that region is becoming less polar.
The contribution of the SA coating to the increase of flexural rigidity is about $|C|_{\text{Flexural rigidity}} = 112.8\%$ which explaines that the coating fills the spaces between the yarns and links the warp and weft threads together, which rigidifies the fabric structure. However, the coating based on SA-EV did not cause any notable modification of wool fabric flexural rigidity.

A significant decrease of the fabric air permeability was noticed after applying the polymeric coating: a decrease of about 20% for Wool- SA and about 38% for Wool-SA-EV.

Based on the accurate findings, it can be concluded that the proposed coating based on sodium alginate and *Eobania Vermiculata* snail shell microparticles is useful and fruitful for future works. Despite the excellent flame retardancy before washing, there was a lack of covalent bonds between the proposed coating and wool keratin polypeptide. In this direction, various process modifications will be explored to improve the treatment durability.

References

Adepitan OL, Alabi OO, Gbadeyan OJ, Deenadayalu N, Jayeola AT (2025) Investigation into the development and utilization of snail shell biomaterials: a systematic review. Discover Mater 5:1. https://doi.org/10.1007/s43939-025-00218-6

Ahmad F, Mushtaq B, Butt FA, Rasheed A, Ahmad S (2021) Preparation and characterization of wool fiber reinforced nonwoven alginate hydrogel for wound dressing. Cellulose 28:7941-7951. https://doi.org/10.1007/s10570-021-04043-x

An F, Fang K, Liu X, Yang H, Qu G (2020) Protease and sodium alginate combined treatment of wool fabric for enhancing inkjet printing performance of reactive dyes. Int J Biol Macromol 146:959-964. https://doi.org/10.1016/j.ijbiomac.2019.09.220

Azam F, Ali S, Ahmad F, Ahmad S, Rasheed A, Shahwan M (2024) Novel waste wool fabric reinforced alginate-gum hydrogel composites for rapid and selective Pb(II) adsorption. Carbohydr Polym Technol Appl 8:100601.
https://doi.org/10.1016/j.carpta.2024.100601

Belukhina O, Milasiene D, Ivanauskas R (2021) Investigation of the possibilities of wool fiber surface modification with copper selenide. Mater 14:1648.
https://doi.org/10.3390/ma14071648

Cardamone JM (2013) Protein-based fibers and fire resistance. In: Selcen KF (ed) Handbook of Fire Resistant Textiles. Woodhead Publishing, Cambridge, pp 246-270.

Cheng XW, Zhang WX, Wu YX, Ma YD, Xu JT, Guan JP (2021) Borate functionalized caramel as effective intumescent flame retardant for wool fabric. Polym Degrad Stab 186:109469. https://doi.org/10.1016/j.polymdegradstab.2020.109469

Cheng XW, Wang ZY, Jin WJ, Guan JP (2022) Covalent flame retardant functionalization of wool fabric using ammonium phytate with improved washing durability. Ind Crops Prod 187:115332. https://doi.org/10.1016/j.indcrop.2022.115332

Diharjo K, Gapsari F, Andoko A, Wijaya MN, Rangappa SM, Siengchin S (2024) Flammability and thermal resistance of Ceiba petandra fiber reinforced composite with snail powder filler. Polym Compos 45:4947-4960.
https://doi.org/10.1002/pc.28100

Flambard X, Bourbigot S, Kozlowski R, Muzyczek M, Mieleniak B, Ferreira M, Vermeulen B, Poutch F (2005) Progress in safety, flame retardant textiles and flexible fire barriers for seats in transportation. Polym Degrad Stab 88:98-105.
https://doi.org/10.1016/j.polymdegradstab.2004.02.024

Frent OD, Vicas LG, Duteanu N, Morgovan CM, Jurca T, Pallag A, Muresan ME, Filip SM, Lucaciu RL, Marian E (2022) Sodium alginate—natural microencapsulation material of polymeric microparticles. Int J Mol Sci 23:12108.
https://doi.org/10.3390/ijms232012108

Haddaji K, Cheriaa R, Jaouachi B (2025) Flame retardancy of cotton fabric based on Eobania vermiculata snail shells. Chem Afr 3:1075-1084.
https://doi.org/10.1007/s42250-025-01198-z

Hassan MM (2018) Wool fabrics coated with an anionic Bunte salt terminated polyether: physicomechanical properties, stain resistance, and dyeability. ACS Omega 3:17656-17667.
https://doi.org/10.1021/acsomega.8b02040

Islam T, Shikder AAR, Hossen MS, Uddin MM, Hossain MT, Bashar MM (2024) Nature-derived flame retardant for cotton fabrics with green coconut shells. J Chem Health Saf 32:57-65.
https://doi.org/10.1021/acs.chas.4c00050

Ivanovska A, Milošević M, Lađarević J, Tarbuk A, Svirčev Z, Kostić M (2024) The impact of sodium periodate oxidation and alginate coating on the capillarity of jute fabric. J Eng Fibers Fabr 19:1-10.
https://doi.org/10.1177/15589250241246071

Janarthanan M, Senthil Kumar M (2019) Extraction of alginate from brown seaweeds and evolution of bioactive alginate film coated textile fabrics for wound healing application. J Ind Text 48:2150-2165.
https://doi.org/10.1177/1528083718783331

Jaouachi B, Cheriaa R, Bouallagui N (2021) Evaluating the effectiveness of coating knitted fabrics with silica nanoparticles for protection from needlestick injuries. J Ind Text 51(2_suppl):3372S-3392S.
https://doi.org/10.1177/15280837211001352

Karaoui M, Hsissou R, Alami M, Assouag M (2023) Physico-chemical characterization of snail shells powder prepared by mechanochemical processes and thermal treatment. J Met Mater Miner 33(2):139-147.
https://doi.org/10.55713/jmmm.v33i2.1700

Linhares T, Carneiro VH, Pessoa de Amorim MT, Durães L (2023) A comparative thermoacoustic insulation study of silica aerogels reinforced with reclaimed textile fibres: cotton, polyester and wool. Gels 9:548.
https://doi.org/10.3390/gels9070548

Malucelli G (2020) Sol-Gel and layer-by-layer coatings for flame-retardant cotton fabrics: recent advances. Coatings 10:333.
https://doi.org/10.3390/coatings10040333

Mariadoss AVA, Wang W-L, Yang C-J, Lai J-Y, Yao C (2026) Snail as a multifunctional biological resource: nutritional value and pharmacological applications. Food Res Int 223:117872.
https://doi.org/10.1016/j.foodres.2025.117872

Mathur P, Sheikh JN, Sen K (2020) Durable flame-retardant wool using sulphamic acid. Polym Degrad Stab 174:109101.
https://doi.org/10.1016/j.polymdegradstab.2020.109101

Parveen S, Chakraborty A, Chanda DK, Pramanik S, Barik A, Aditya G (2020) Microstructure analysis and chemical and mechanical characterization of the shells of three freshwater snails. ACS Omega 5:25757-25771.
https://doi.org/10.1021/acsomega.0c03064

Peceño B, Alonso-Fariñas B, Vega G, Carrizo D, Leiva C (2025) Sustainable fire-resistant materials: thermal, physical, mechanical, and environmental behavior of walls with waste from the aquaculture industry. Materials 18:5086.
https://doi.org/10.3390/ma18225086

Ren Y, Shi J, Wang D, Liu J, Wang Z, Guo Q, Wang H (2026) Efficient and durable flame-retardant wool fabrics achieved by a facile phytic acid grafting approach. Polymer 342:129336.
https://doi.org/10.1016/j.polymer.2025.129336

Rungpin N, Pavasupree S, Prasassarakich P, Poompradub S (2015) Production of nano-calcium carbonate from shells of the freshwater channeled applesnail, Pomacea canaliculata, by hydrothermal treatment and its application with polyvinyl chloride. Polym Compos 36:1620-1628.
https://doi.org/10.1002/pc.23070

Sadeghi-Kiakhani M, Safapour S, Habibzadeh SA, Tehrani-Bagha AR (2021) Grafting of wool with alginate biopolymer/nano Ag as a clean antimicrobial and antioxidant agent: characterization and natural dyeing studies. J Polym Environ 29:2639-2649.
https://doi.org/10.1007/s10924-021-02046-0

Salmeia KA, Gaan S, Malucelli G (2016) Recent advances for flame retardancy of textiles based on phosphorus chemistry. Polymers 8:319.
https://doi.org/10.3390/polym8090319

Sethi SK, Manik G (2018) Recent progress in super hydrophobic/hydrophilic self-cleaning surfaces for various industrial applications: a review. Polym-Plast Technol Eng 57:1932-1952.
https://doi.org/10.1080/03602559.2018.1447128

Shahidi S, Ghoranneviss M, Dalalsharifi S (2015) Preparation of multifunctional wool fabric using chitosan after plasma treatment. J Text Inst 106:1127-1134.
https://doi.org/10.1080/00405000.2014.977522

Sharma A, Singh AK (2025) Sodium alginate: a green biopolymer resource-based antimicrobial edible coating to enhance fruit shelf-life: a review. Colloids Interfaces 9:32.
https://doi.org/10.3390/colloids9030032

Shikder AAR, Mamun MA, Islam T, Khan MHK, Uddin MZ (2023) Fire retardant properties enhancement of cotton twill fabric using pumpkin (Cucurbita maxima) extract. Heliyon 9:e14806.
https://doi.org/10.1016/j.heliyon.2023.e14806

Su C-H, Kumar GV, Adhikary S, Velusamy P, Pandian K, Anbu P (2017) Preparation of cotton fabric using sodium alginate-coated nanoparticles to protect against nosocomial pathogens. Biochem Eng J 117:28-35.
https://doi.org/10.1016/j.bej.2016.10.020

Sykam K, Försth M, Sas G, Restás Á, Das O (2021) Phytic acid: a bio-based flame retardant for cotton and wool fabrics. Ind Crops Prod 164:113349.
https://doi.org/10.1016/j.indcrop.2021.113349

Szczepanik E, Molik E, Pielichowska K (2025) Polysaccharide hydrogels with waste wool fibre as matrix for potential use as CRF fertiliser. Molecules 30:2885.
https://doi.org/10.3390/molecules30132885

Wang H, Guo S, Zhang C, Qi Z, Li L, Zhu P (2021) Flame retardancy and thermal behavior of wool fabric treated with a phosphorus-containing polycarboxylic acid. Polymers 13(23):4111.
https://doi.org/10.3390/polym13234111

Wang H, Liu J, Fan X, Ren J, Liu Q, Kong B (2022) Fabrication, characterisation, and application of green crosslinked sodium alginate hydrogel films by natural crab-shell powders to achieve drug sustained release. LWT-Food Sci Technol 171:114147.
https://doi.org/10.1016/j.lwt.2022.114147

Wang H, Qiu Q-L, Li B, Yu H, Xu L, Qiu J (2025) Alginate-based flame-retardant coatings for sustainable fire protection: a review. Int J Biol Macromol 308:142448.
https://doi.org/10.1016/j.ijbiomac.2025.142448

Wulandari AP, Karlina E, Tanudjaja E, Rohmat A, Kusmoro J, Fadhlillah M, Somantri K, Sahroni R, Fatriasari W (2024) Characteristics and quality of flame-retarded ramie fabrics for the development of functional textiles. Mater 17:1416.
https://doi.org/10.3390/ma17061416

Xu J, Jiang S, Peng L, Wang Y, Shang S, Miao D, Guo R (2019) AgNps-PVA-coated woven cotton fabric: preparation, water repellency, shielding properties and antibacterial activity. J Ind Text 48:1545-1565.
https://doi.org/10.1177/1528083718764908

Zhang H, Sun R, Wu H, Mao N (2018) Enhanced photocatalytic activity of wool fibers having titanium dioxide nanoparticles formed inside their cortex. Nanotechnology 29:295606.
https://doi.org/10.1088/1361-6528/aac1b3

Statements & Declarations

Acknowledgements

“This is not applicable' for that specific section”.

Funding

“The authors declare that no funds, grants, or other support were received during the preparation of this manuscript.”

Author’s Contributions

“The manuscript was written through contributions of all authors. All authors contributed to the study steps. Material preparation, data collection and analysis were performed by Khadija Haddaji, Soumaya Tabib. Supervision were performed by Rim Cheriaa and Boubaker Jaouachi. The first draft of the manuscript was written by Khadija Haddaji and Rim Cheriaa and all authors commented on previous versions of the manuscript. All authors read and approved the final manuscript”.

Ethical Approval

“This article does not contain any studies with human participants or animals performed by any of the authors. Therefore, ethical approval is not applicable' for that specific section”.

Consent to Participate

“Not applicable for that specific section, as the study did not involve human participants”.

Consent to Publish

“All the authors have approved the manuscript for publication”.

Competing Interests

"The authors declare no competing interests".

Data Availability Statement

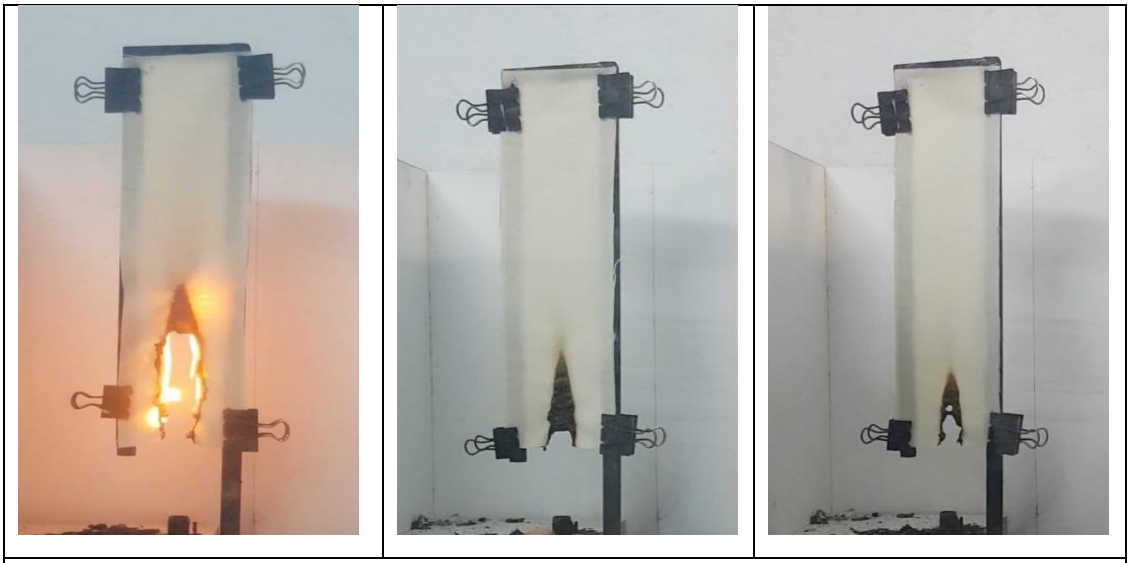
"The data supporting the findings of this study are available within the paper. Any additional data required can be obtained from the corresponding author upon request.".

Table 6. Coated wool fabrics caracteristics and sample code

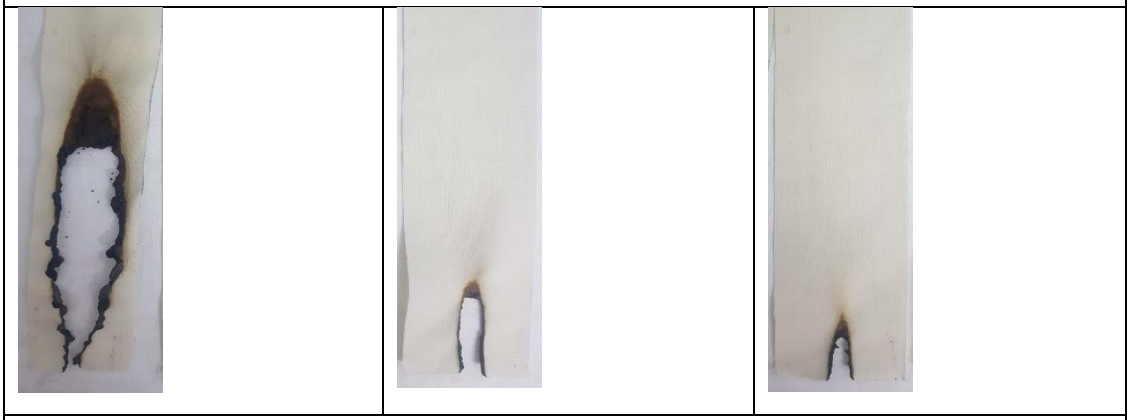
Sample ID	**Sodium alginate powder concentration, g/L**	**Snail shell microparticles concentration, g/L**	**Add on, %**
Wool-NT	0	0	0.00
Wool-SA	25	0	1.65 ± 5.01 (*)
Wool-SA-EV	25	20	5.41 ± 1.98
(*) Mean value ± standard deviation			

Table 7. Photos of uncoated and coated wool fabrics

Wool-NT	**Wool-SA**	**Wool-SA-EV**



(a) At the time of flame removal (12s)



(b) Vertical flame test final results

Table 8. Flammability testing results

Sample	Afterflame time, s	Char length, cm	Observed burning rate, cm/s
Wool-NT	32.17 ± 0.52 (*)	27.53 ± 4.27	0.86 ± 0.33

Wool-SA	0.00 ± 0.00	7.5 ± 0.84	--
Wool-SA-EV	0.00 ± 0.00	5.4 ± 0.03	--
Washed Wool-SA-EV	30.40 ± 0.46	25.5 ± 0.02	0.96 ± 0.44

(*) Mean value ± standard deviation

Table 9. Comparative flexural rigidity results and structural properties

Sample	**Thickness, (mm)**	**Mass per unit area, (g/m^2)**	**Bending length (**), (cm)**		**Flexural rigidity, (mg.cm)**
			Coated side	**Uncoated side**	
Wool-NT	0.502 ± 0.002(*)	223.83 ± 1.75	1.06 ± 0.04	1.17 ± 0.08	3.10 ± 0.50
Wool-SA	0.553 ± 0.003	225.7 ± 0.53	1.5 ± 0.05	1.36 ± 0.03	6.59 ± 0.56
Wool-SA-EV	0.554 ± 0.002	235.74 ± 2.13	1.18 ± 0.03	1.17 ± 0.09	3.82 ± 0.51

(*) Mean value ± standard deviation

(**) Bending length measured in warp direction (the coating direction)

Table 10. Air permeability test results

Sample	**Air permeability,** L/m^2/s
Wool-NT	267.00 ± 5.15 (*)
Wool-SA	212.33 ± 3.53
Wool-SA-EV	165.33 ± 5.95

(*) Mean value ± standard deviation

Figure captions

Fig. 2 Schematic illustration of coating process

Fig. 3 SEM images of uncoated and coated wool fabrics: (a) Wool-NT (×40), (b) Wool-SA (×40), (c) Wool-SA-EV (×40), (d) Wool-SA-EV (×90)

Fig. 4 FTIR analysis of sodium alginate powder

Fig. 5 FTIR analysis of *Eobania Vermiculata* snail shell

Fig. 6 FTIR analysis of uncoated and coated wool fabrics

Fig. 7 Tensile strength testing results (warp direction): (a) Tensile curve, (b) Maximum force, (c) Elongation at maximum force

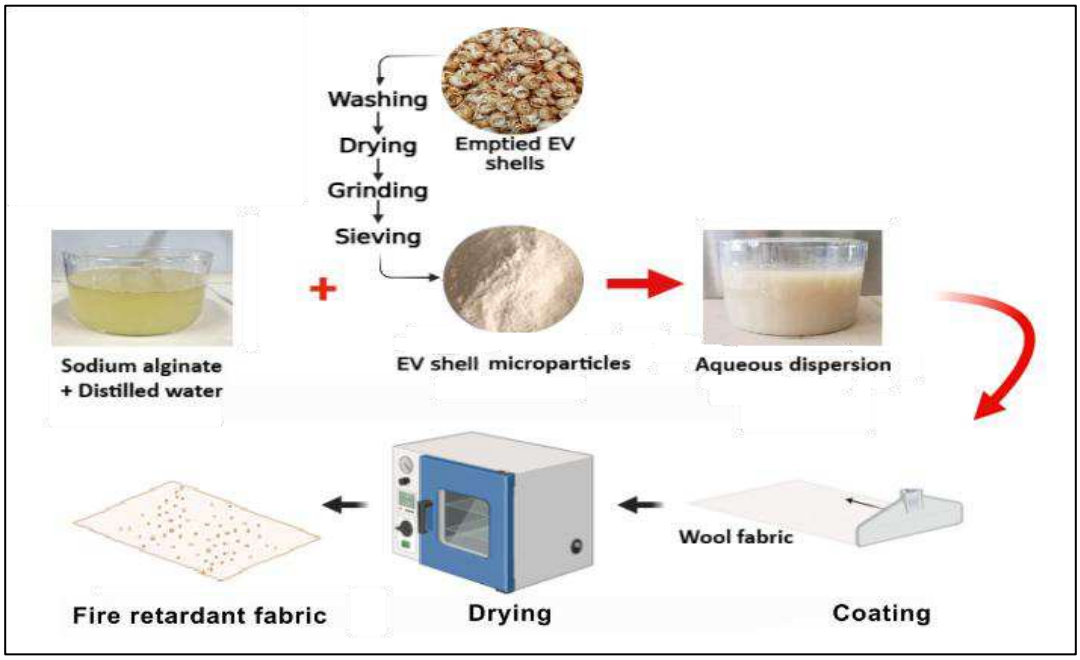
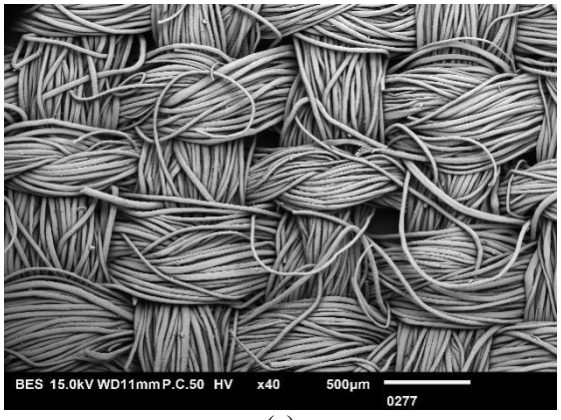
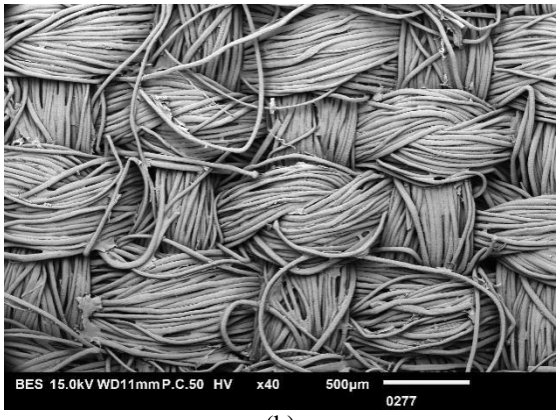


Fig.1 Schematic illustration of coating process



(a)



(b)



(c) (d)

Fig. 2 SEM images of uncoated and coated wool fabrics:

(a) Wool-NT (×40), (b) Wool-SA (×40), (c) Wool-SA-EV (×40), (d) Wool-SA-EV (×90)

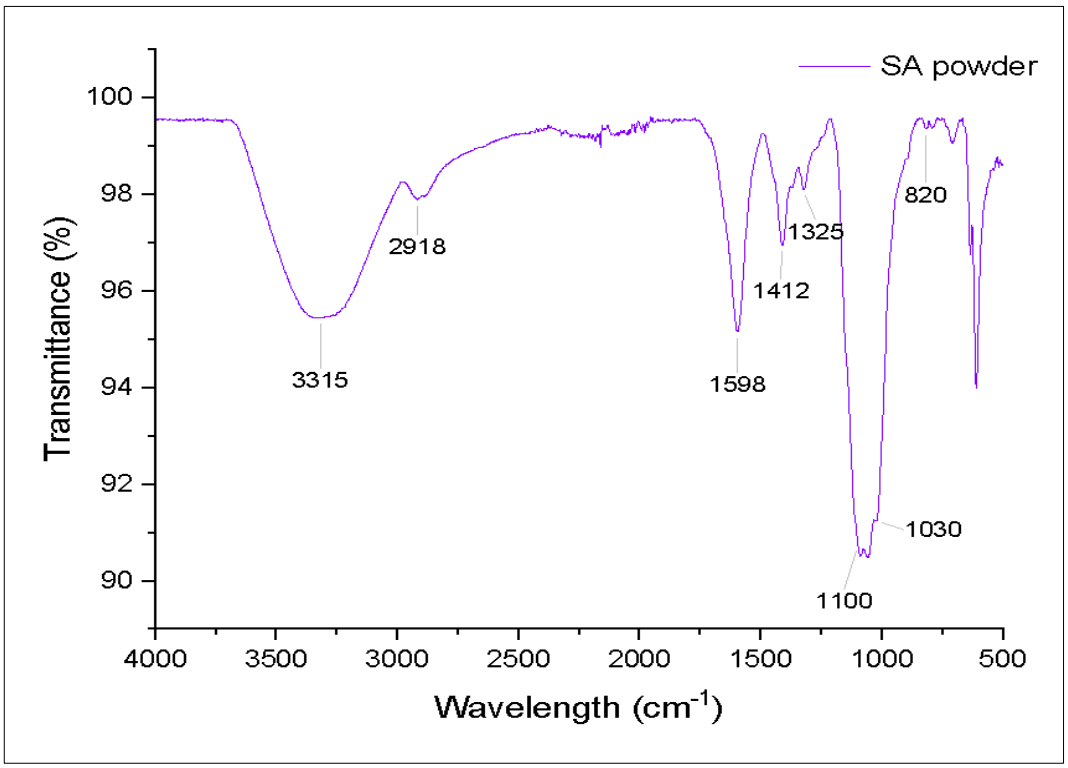


Fig. 3 FTIR analysis of sodium alginate powder

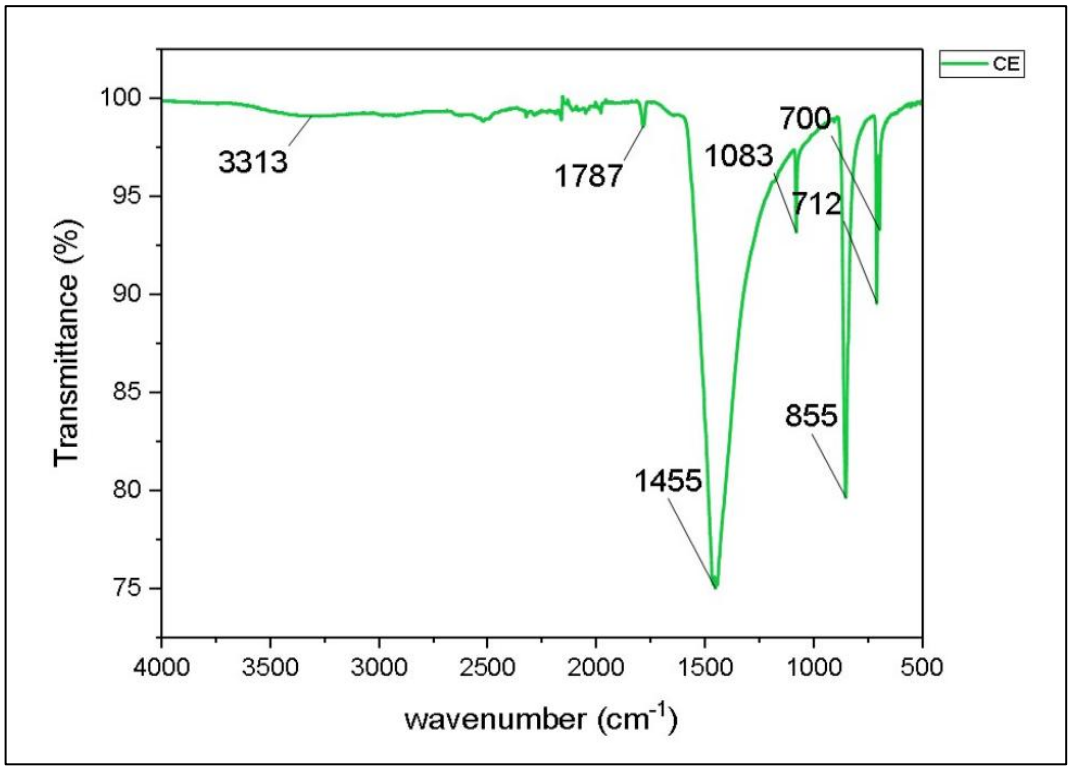


Fig. 4 FTIR analysis of *Eobania Vermiculata* snail shell

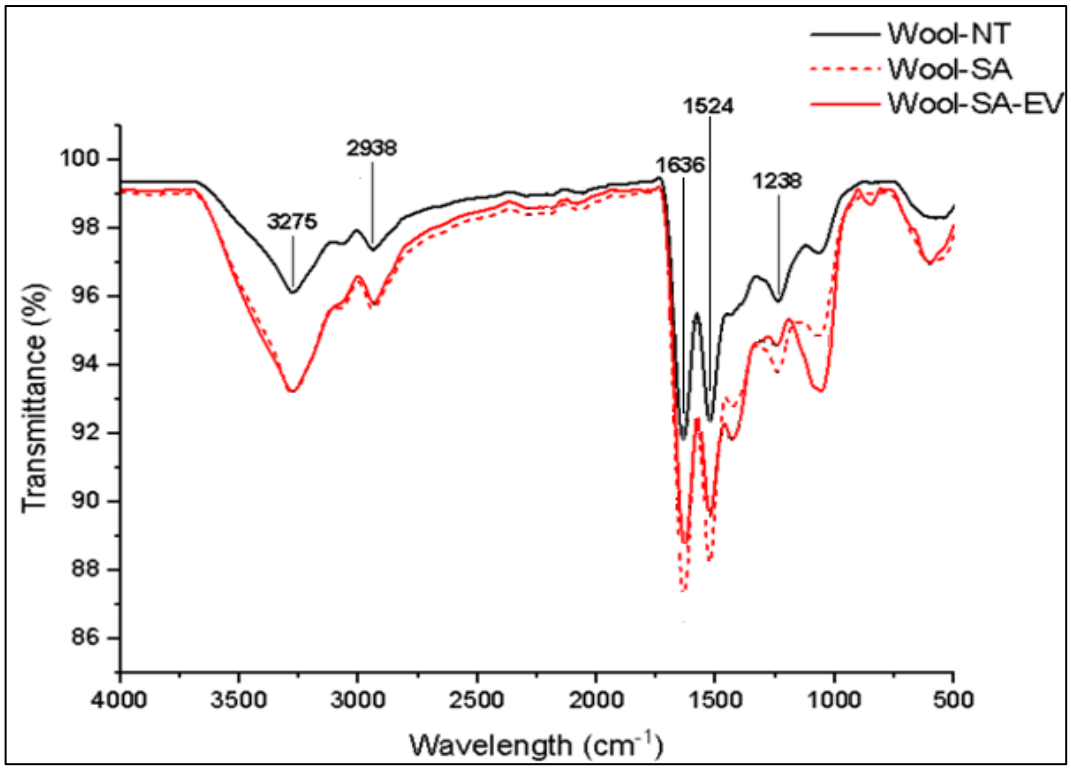


Fig. 5 FTIR analysis of uncoated and coated wool fabrics

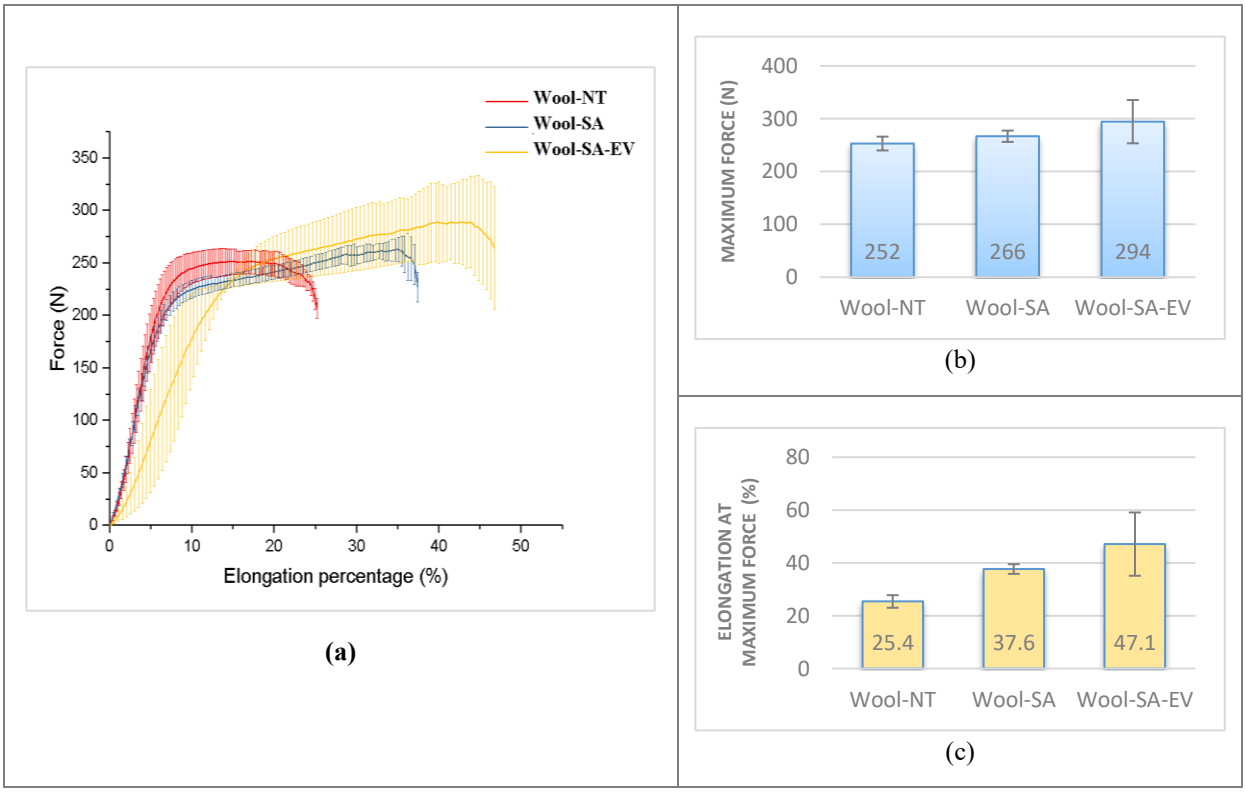


Fig. 6 Tensile strength testing results (warp direction):

(a) Tensile curve, (b) Maximum force, (c) Elongation at maximum force